Journal of Membrane Science 685 (2023) 121938

Contents lists available at ScienceDirect

Journal of Membrane Science

journal homepage: www.elsevier.com/locate/memsci

Mixed matrix iongel membranes containing azo-porous organic polymers: Influence of temperature, pressure and water vapour on CO_2 separation

Ana R. Nabais [a], Paloma Ortiz-Albo [a], Jin-Xiu Zhou [b], Mu-Hua Huang [c], David Mecerreyes [b,d], João G. Crespo [a], Liliana C. Tomé [a,**], Luísa A. Neves [a,*]

[a] LAQV-REQUIMTE, Department of Chemistry, NOVA School of Science and Technology, FCT NOVA, Universidade NOVA de Lisboa, 2829-516, Caparica, Portugal
[b] POLYMAT, University of the Basque Country UPV/EHU, Avda. Tolosa 72, Donostia-San Sebastian, 20018, Gipuzkoa, Spain
[c] School of Materials Science and Engineering, Beijing Institute of Technology, No. 5, Zhongguancun South Street, Beijing, 100081, China
[d] Ikerbasque, Basque Foundation for Science, 48013, Bilbao, Spain

ARTICLE INFO

Keywords:
Porous organic polymers
Ionic liquids
Mixed matrix iongel membranes
Binary gas mixtures
Water vapour

ABSTRACT

The effect of temperature, pressure, and humidity content in the gas separation performance of iongel membranes are crucial parameters that should be assessed to determine the real potential of these materials to be used in CO_2 separation processes. In this work, we present a detailed study on the impact of temperature (303, 323 and 353 K), pressure (2 and 4 bar), gas composition and water vapour content (between 11 and 21% of relative humidity) on the performance of iongels containing azo-porous organic polymers (azo-POPs), for CO_2/N_2 and CO_2/CH_4 binary gas separations. The iongels combining 80 wt% of the ionic liquid (IL) [C_2mim][TFSI], 20 wt% of poly(ethylene glycol) diacrylate (PEGDA) and 0.5 wt% of different azo-POPs were prepared by a solvent-free UV curing method. At the lower temperature, the pressure increase seems to have a negative impact on the CO_2 permeability of the prepared mixed matrix iongel membranes (MMIMs). However, the opposite behaviour was found when the temperature increases. Moreover, the presence of humidity in the feed gas stream affects the gas separation performance of the studied iongels, since the CO_2 permeability greatly increases with increasing humidity in the gas mixture, while the selectivity decreases, for both gas separations under study. In general, the high pressure and temperature, and the presence of humidity have a significant influence on the separation performance of the studied iongel membranes, due to induced alterations in their structure and overall stability.

1. Introduction

Throughout the years, membrane processes have established themselves as one of the most promising strategies to purify gas streams. Compared to other processes, such as absorption using aqueous amine solutions, pressure swing adsorption and cryogenic distillation, the use of membranes can offer several advantages, namely in terms of energy-saving, continuous operation mode, low maintenance required and the inherent simplicity of the process [1,2]. However, despite the attractiveness of this process, the use of membranes still faces some challenges, namely in terms of the materials used. Ideally, high membrane permeance (ratio between permeability and membrane thickness) is always the target along with an optimal value of selectivity that will depend on the operating pressure and process design [3]. Although different membrane materials have been used, all the current commercially available membranes for gas separation (CO_2/N_2) are polymeric membranes. For instance, Polaris™ (MTR) and PolyActive™ (Hereon) present CO_2 permeances of 2200 and 1450 GPU and CO_2/N_2 selectivities of 50 and 46, respectively, which can be regarded as target values in terms of membrane separation performance [4].

The challenging experimental conditions of some of the most common industrial gas separations, either in terms of temperature, pressure, or separation performance requirements, may represent a setback in the development of membrane processes at large scale [3]. Therefore, the performance of membranes in harsh industrial conditions (e. g. high pressure and high temperature, see Table 1) should be properly assessed before the process can be scaled up.

The pressure increase, for example, in natural gas and syngas streams, might have a significant effect on the membranes' separation performance, especially if highly condensable gases such as CO_2 and

* Corresponding author.
** Corresponding author.
E-mail addresses: liliana.tome@fct.unl.pt (L.C. Tomé), lan11892@fct.unl.pt (L.A. Neves).

https://doi.org/10.1016/j.memsci.2023.121938
Received 17 April 2023; Received in revised form 21 June 2023; Accepted 14 July 2023
Available online 15 July 2023

Table 1
Typical conditions of the CO_2/N_2 and CO_2/CH_4 industrial gas streams.

	Separation	Temperature (K)	Pressure (bar)	References
Flue gas	CO_2/N_2	308–393	1	[5–8]
Natural Gas	CO_2/CH_4	298–308	30–50	[8–10]
Biogas	CO_2/CH_4	298–308	1	[8,11]

heavy hydrocarbons are present in the gas mixture. Highly sorbing gases can induce swelling of the polymer chains, also known as plasticization, leading to a significant increase of the fractional free volume and gas diffusion rate. As a consequence of the higher gas diffusivity, the gas permeability increases while selectivity usually decreases [12]. On the other hand, depending on the membrane's material, elevated temperatures can also have a significant impact on the membranes' separation performance, usually by increasing the permeability at the expense of the gas selectivity [13]. Besides the effect of pressure and temperature, the presence of water vapour in some gas streams can also influence the separation performance of membranes. The presence of water molecules in the gas stream can lead to the formation of water clusters that fill the membranes' free volume or promotes a competitive sorption effect with other gas molecules, decreasing their permeability. The opposite effect can also be observed if the water vapour molecules are able to change the membrane's structure by inducing a plasticization effect [14].

The selection of the most suitable materials to fabricate membranes for gas separation is the key factor behind a successful separation performance, under harsh conditions. In the last few years, a variety of new materials have been proposed as alternatives to prepare membranes with superior gas separation performance. Among them, ionic liquid (IL)-based membranes have been looked at as one of the most versatile classes of materials that can be used to achieve high gas separation performances [15]. These materials take advantage of, not only their high affinity for specific gases, such as CO_2, but a high thermal and chemical stability [16–18]. In particular, iongel membranes, containing a high amount of IL and a polymer network to provide the necessary mechanical support, can take benefit from these intrinsic IL properties, to achieve high gas permeabilities and selectivities [19–23]. To improve the separation performance of these iongels, a third component, such as metal organic frameworks (MOFs), zeolites and silica particles, can also be added to prepare MMIMs [24]. Over the past years, the development of MMIMs has shown promising results towards the separation of CO_2. Noble's group carried out pioneer work regarding mixed matrix membranes with zeolite particles, such as SAPO-34, poly(ionic liquid)-based membranes and moderate contents of [C_2mim][TFSI] IL, for CO_2/N_2 and CO_2/CH_4 separations [25–28]. Even though the membranes prepared by the authors do not fall under the definition of iongel considered in this work, the results showed that there was a clear advantage when combining a solid filler with an IL, unveiling the potential of using MMIMs for gas separation. Later on, Matsuyama's group developed silica containing iongel membranes, with not only good separation performances but also remarkable mechanical properties, able to withstand up to 28 MPa of compressive stress [29–31]. Moreover, we studied the influence of different MOFs (MOF-5, Cu(BTC), MIL-53 and ZIF-8) loadings and ILs ([C_2mim][BETI] and [C_4mpyr][Tf_2N]) incorporated in poly([pyr_{11}][TFSI]-based membranes for CO_2 separation. It was clear that the CO_2 permeability was significantly improved, however at the expense of the ideal selectivity [32,33]. Following a similar approach, a nanoclay (Nanomer®1.34TCN, montmorillonite – MMT) was used to reinforce poly(ethylene glycol) diacrylate (PEGDA) iongel membranes in a self-standing form. The additional mechanical resistance provided by the inorganic particles, at 7.5 wt% loading, allowed for the preparation of free-standing iongels with 80 wt% [C_2mim][TFSI] IL and an increase in permeability and in CO_2/N_2 and CO_2/CH_4 ideal selectivities, due to the higher IL content [34].

More recently, azo-porous organic polymers (azo-POPs) have also attracted much attention regarding their potential towards CO_2 separation applications [35–40]. The use of totally organic fillers such as azo-POPs combined with ILs, can help to overcome the compatibility issues between the filler particles and the polymer materials, which is known for being one of the main challenges regarding the fabrication of mixed matrix membranes. We recently reported an efficient synthetic pathway to prepare four different azo-POPs (azo-POP-1, azo-POP-10, azo-POP-11 and azo-POP-12) to be used as fillers and improve the CO_2 separation performance of PEGDA iongel membranes bearing [C_2mim][TFSI] IL [41]. The results obtained in pure gas permeation experiments showed a considerable improvement on the iongels' permeability and selectivity upon the incorporation of azo-POP-1 and azo-POP-11 [41]. However, the performance of MMIMs under conditions similar to those of the most relevant industrial gas streams (Table 1) is yet to be fully assessed [24]. In this work, we started by evaluating the influence of different water activities in the pure gas permeation of the iongel membranes containing the different azo-POPs. Additionally, we evaluated the CO_2/N_2 and CO_2/CH_4 separation performance of the previously proposed MMIMs iongels containing azo-POP-1 and azo-POP-11 under different experimental conditions. To make a more realistic evaluation, the effect of temperature, pressure, gas composition and presence of water vapour on the iongels' performance was assessed.

2. Experimental

2.1. Materials

Poly(ethylene glycol) diacrylate (PEGDA, M_n 575 g mol^{-1}) and 2-hydroxy-2-methylpropiophenone (DAROCUR®, 97 wt% pure) were purchased from Sigma-Aldrich (Portugal). Ionic liquid 1-ethyl-3-methylimidazolium bis(triuoromethylsulfonyl) imide ([C_2mim][TFSI], 99 wt% pure) was supplied by Iolitec GmbH (Germany). Carbon dioxide, CO_2 (99.998% purity), nitrogen, N_2 (99.99% purity), methane, CH_4 (99.99% purity) and helium, He (>99% purity) gases were provided by Praxair (Portugal). Azo-POP-1, azo-POP-10, azo-POP-11 and azo-POP-12 were synthesized according to a previously described procedure [41]. The characterization of the different azo-POPs, including the determination of the BET surface area, porous volume, mean pore size and CO_2 adsorption capacity, can be found in our previous work [41].

2.2. Preparation of mixed matrix iongel membranes (MMIMs)

The MMIMs containing azo-POP-1 (designated as PEGDA-80 TFSI-0.5 POP-1), azo-POP-10 (designated as PEGDA-80 TFSI-0.5 POP-10), azo-POP-11 (designated as PEGDA-80 TFSI-0.5 POP-11) and azo-POP-12 (designated as PEGDA-80 TFSI-0.5 POP-12) were tested in this work [41]. The iongels were prepared by mixing 0.5 wt% (above the total iongel mass) of the selected azo-POP with 80 wt% of [C_2mim][TFSI] IL and left stirring overnight. Subsequently, 20 wt% of PEGDA was added and the solution was left stirring for 1 more hour before adding 3 wt% (relative to PEGDA mass) of DAROCUR® as photoinitiator. The final solution was placed on top of hydrophilic polyamide (PA) support (Sartorius™, supplied by Fisher Scientific), with a pore size of 0.22 μm and then between two Rain-X® coated quartz plate, with a 100 μm spacer in between. The hydrophilic porous support was subjected to a pre-wetting step before the iongel casting, to minimize pore filling. The final set was exposed to a UV light using a UVP Cross-linker CL-3000 (Analytik Jena, Germany), with a wavelength of 365 nm and an intensity of 1.9 mW cm^{-2} for 10 min. Before testing, the resulting membranes were then dried at 333 K to remove the water trapped inside the polymer support. The temperature and time needed to dry the support was confirmed by weighing the membrane before immersion in water and after the drying step, being considered dried when a constant support weight was obtained. Therefore, it was considered that the permeability results obtained in this work, from the pure and mixed gas permeation experiments, correspond to the iongel layer without the

resistance of the porous support (as it was confirmed when trying to perform permeation experiments on the support alone and no resistance to gas transport was observed). This means that, in the present work, it was not necessary to use the Resistance in Series Model (RSM) as previously reported [41]. A schematic representation of the fabrication of the MMIMs can be found in Fig. 1.

2.3. Effect of water activity

The prepared iongels were conditioned at different water activities (a_w). Saturated salt solutions were used to equilibrate the iongel membranes at a defined water activity through the vapour phase, as listed in Table 2. Specific amounts of different inorganic salts were mixed with distilled water and the iongels were placed in four different desiccators, each with a well-defined water activity at 303 K. A thermohygrometer equipped with a HM42 probe (Vaisala, Finland) was used to confirm the RH inside each desiccator. The weight and thickness of each sample were measured every 5 days until these parameters remained constant, after approximately 3 weeks, meaning that the iongels were equilibrated at the desired RH before being tested for pure and mixed gas experiments.

2.4. Gas permeation

2.4.1. Pure gases

Pure gas permeation experiments were carried out for pure CO_2, N_2 and CH_4, to evaluate the influence of the presence of water inside the iongels structure on their separation performance, according to a previously described procedure [43]. The iongel membranes were placed inside a stainless-steel permeation cell divided into two compartments, specified as feed and permeate. The cell was placed inside a water bath, with a controlled temperature of 303 K. All permeation experiments were performed at a transmembrane pressure of 0.7 bar of relative pressure, and three replicates of each membrane were tested. Two different replicates of each membrane were tested, and the mean value and standard error (calculated by dividing the standard deviation of the samples by the square root of the sample size) were calculated.

Table 2
Saturated salt water activities, at 303 K [42].

Salt	Water activity (a_w)
Lithium chloride, LiCl	0.113
Potassium acetate, CH_3CO_2K	0.216
Sodium bromide, NaBr	0.560
Sodium chloride, NaCl	0.751

The permeability of the pure gas through the iongel membrane equilibrated at the desired RH was calculated from the acquired pressure data over time, on both compartments, according to the following equations:

$$\frac{1}{\beta}\ln\left(\frac{[p_{feed}-p_{perm}]_0}{[p_{feed}-p_{perm}]}\right)=\frac{1}{\beta}\ln\left(\frac{\Delta p_0}{\Delta p}\right)=P\,\frac{t}{l} \quad (1)$$

Where Δp_0 and Δp (bar) represent the pressure variations, at time zero and over time, respectively, between the feed and permeate compartments of the cell, P (m^2s^{-1}) is the permeability of the iongel membrane towards a specific gas (where 1 Barrer = $1x10^{-10}$ cm^3 cm cm^{-2} s^{-1} $cmHg^{-1}$ = $8.3x10^{-13}$ m^2 s^{-1}) [44], t is the time (s) and l is the iongel layer thickness (m). β (m^{-1}) is a geometric parameter, characteristic of the geometry of the cell, given by:

$$\beta = A\left(\frac{1}{V_{feed}}+\frac{1}{V_{perm}}\right) \quad (2)$$

Where A is the iongel active membrane area (m^2) and V_{feed} and V_{perm} are the volumes (m^3) of the feed and permeate compartments, respectively. The permeability of the iongel membrane was obtained from the slope represented by plotting $\frac{1}{\beta}\ln\left(\frac{p_0}{p}\right)$ versus $\frac{t}{l}$.

The ideal gas selectivity was calculated by dividing the permeabil-

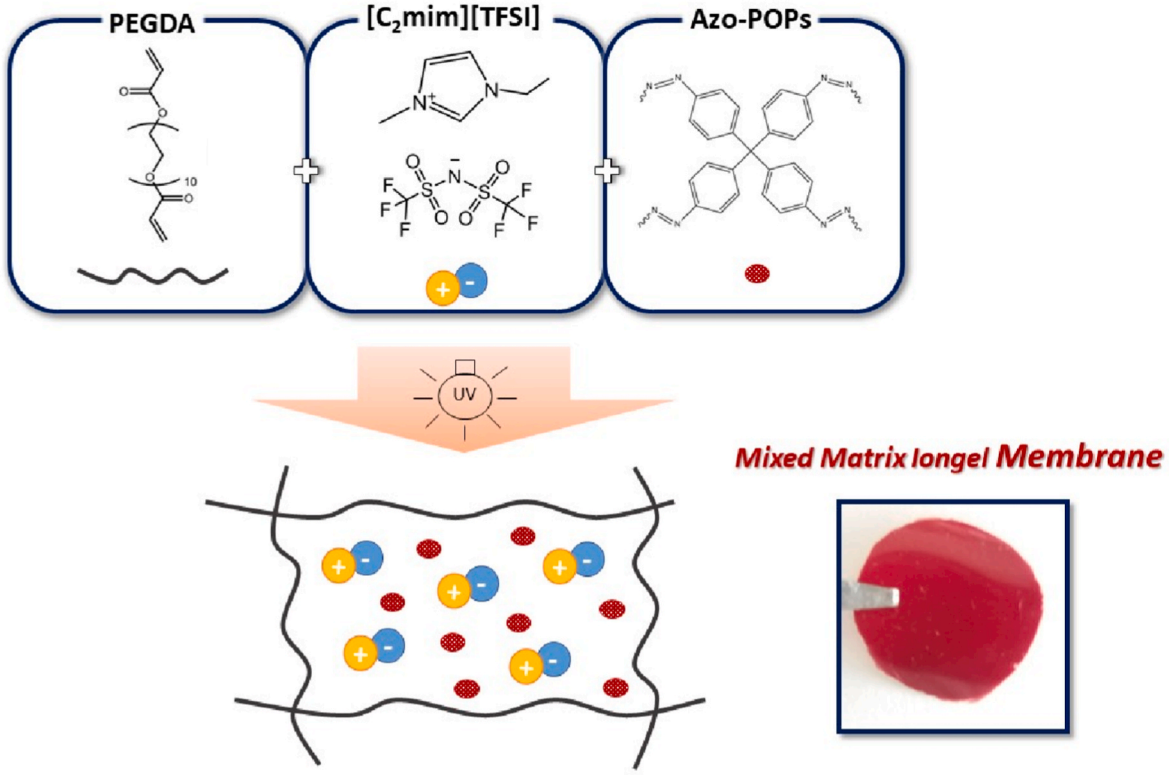

Fig. 1. Schematic representation of the preparation of the MMIMs studied in this work.

ities of the two tested gases (*A* and *B*), according to:

$$\alpha_{A/B} = \frac{P_A}{P_B} \quad (3)$$

2.4.2. Binary gas permeation experiments

Binary gas mixture experiments for CO_2/N_2 and CO_2/CH_4 mixtures were performed using an experimental set-up, schematically represented in Fig. 2, to determine the permeability and real selectivity of the prepared iongel membranes, under mixed gas conditions. The setup is composed by a stainless-steel cell, divided in two compartments (feed and permeate) separated by the membrane to be tested, placed inside an oven (Venticell MMM, Germany) with a controlled temperature (TC). The flow rate of each gas (CO_2 and N_2 or CH_4) was controlled by two mass flow controllers, MFC1 and MFC2 (Alicat Scientific, USA) connected to the gas bottles, which were then mixed, inside the oven, before entering the feed compartment of the membrane module. The experimental pressure was controlled by a back pressure regulator (BPR). Helium (He) was used as sweep gas on the permeate compartment (MFC3) during the experiment, with a flow rate of 5 mL min^{-1} and pressure around 1 bar. The flow rate of the permeate stream was measured by a mass flow meter, MFM (Alicat Scientific, USA). The gas flow rate was obtained directly from the MFM, where only He sweep gas was detected since the flow rate of the gases passing on the permeate compartment was too low to be sensed.

Retentate and permeate compositions were analysed using an Agilent gas chromatograph (GC) 7890B (in which He was used as the gas carrier), equipped with a thermal conductivity detector (TCD) and maintained at 473 K. For the analysis, an isothermal method was used, with a PoraPlot U column connected to a Molsieve 5A column, purchased from Soquimica Lda. (Lisbon, Portugal). Each experiment was carried out until a constant permeate flow and composition were achieved.

The experiments were carried out at different temperatures, pressures, and gas compositions, as listed in Table 3, to achieve experimental conditions similar to those of flue gas (CO_2/N_2) and biogas upgrading (CO_2/CH_4) streams. Two separate replicates of each membrane were tested under the stated experimental conditions. More specifically, the experiments were conducted according to the following procedure: (i) Constant pressure and temperature, varying the CO_2 composition from the lowest to the highest; (ii) Increase in pressure and constant temperature, varying the CO_2 composition from the lowest to the highest; (iii) Increase in temperature and constant pressure, varying the CO_2 composition from the lowest to the highest. Different samples were used for the various experimental conditions of temperature and pressure, to prevent the effects of previous experimental conditions on the membrane's performance. The same sample was used when only the gas composition was changed. The mean value and standard error (calculated by dividing the standard deviation of the samples by the square root of the sample size) were calculated.

Table 3
Experimental conditions for the binary gas mixture permeation experiments.

Gas stream	Temperature (K)	Pressure (bar)	Gas composition
CO_2/N_2	303, 323 and 353	2 and 4	5-30 vol% CO_2
CO_2/CH_4	303	2 and 4	10-40 vol% CO_2

The permeability of each gas was calculated according to:

$$j_i = \frac{F^p_{total} \cdot y^p_i}{A} \quad (4)$$

$$\Delta p_i = p^f \cdot y^f_i - p^p \cdot y^p_i \quad (5)$$

$$P_i = \frac{j_i \cdot l}{\Delta p_i} \quad (6)$$

Where j_i is the molar flux of gas *i* (mol m^{-2} s^{-1}), *F* is the gas molar flow rate (mol s^{-1}), y^f and y^p are the gas molar fractions on the feed and permeate side, respectively, *A* is the iongel membrane area (m^2), Δp represents the driving force between feed and permeate sides (Pa), p^f and p^p are the pressures (Pa) in the feed and permeate sides, respectively, *l* is the iongel layer thickness (m) and *P* is the iongel membrane permeability towards gas *i* (mol m^{-1} Pa^{-1} s^{-1}).

2.4.3. Humidified mixed gas permeation experiments

The experimental setup schematically represented in Fig. 3 was used

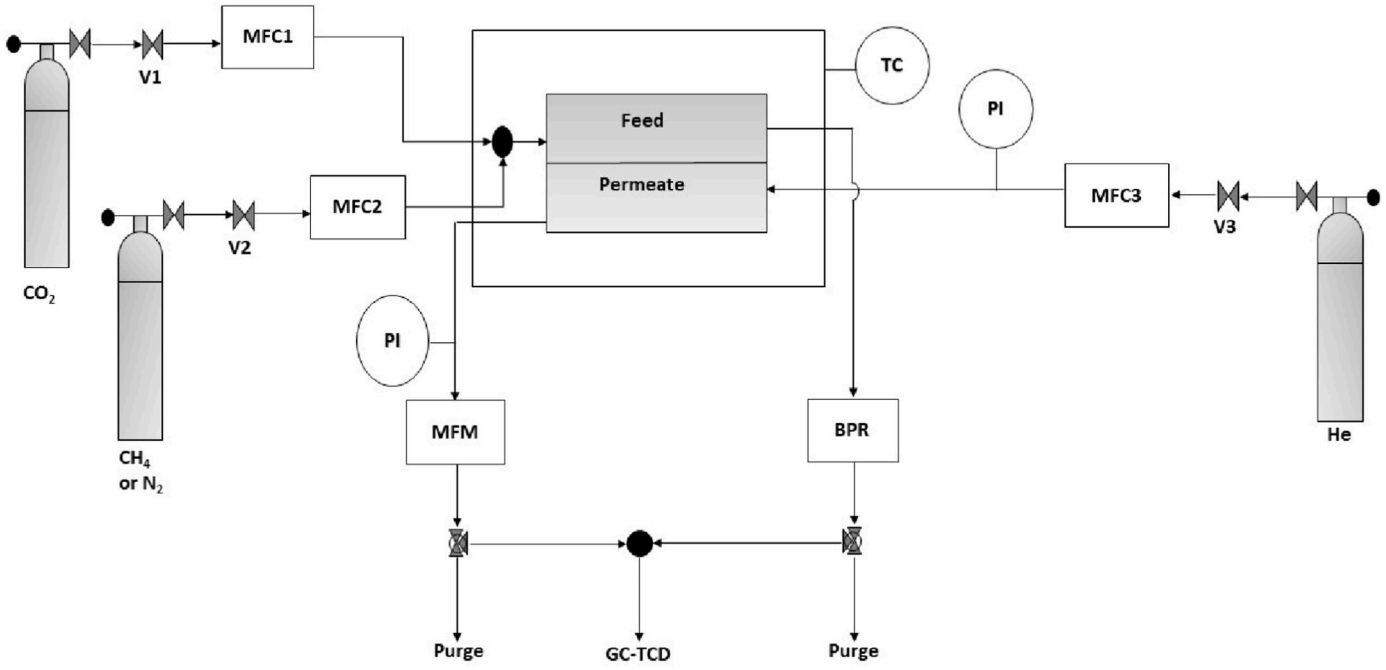

Fig. 2. Schematic representation of the experimental setup used for the mixed gas permeation experiments (dry conditions): BPR – back pressure regulator; MFC1-MFC3 – mass flow controllers; MFM – mass flow meter; PI – pressure indicator; TC – temperature controller; V1–V3 – valves.

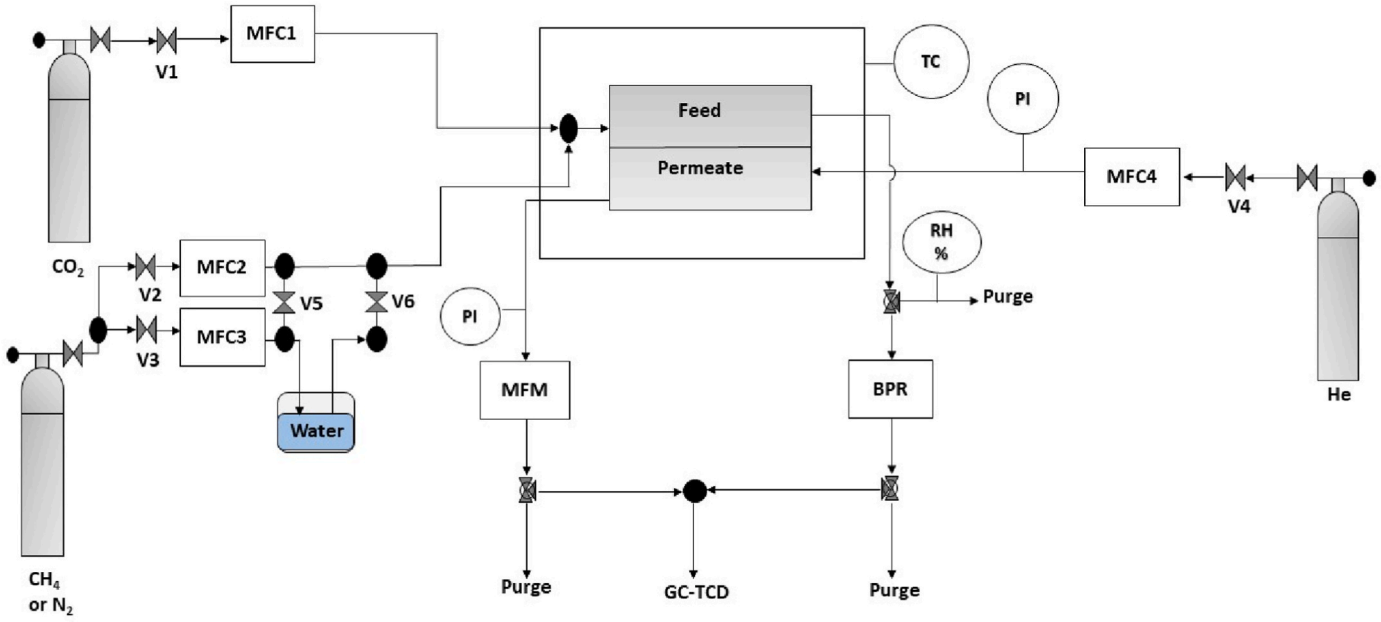

Fig. 3. Schematic representation of the experimental setup used for the mixed gas permeation experiments (humidified conditions): BPR – back pressure regulator; MFC1-MFC4 – mass flow controllers; MFM – mass flow meter; PI – pressure indicator; RH% - relative humidity indicator; TC – temperature controller; V1–V6 – valves.

to evaluate the effect of relative humidity (RH) present in the stream on the gas separation of the iongels membranes, under mixed gas conditions. To obtain a humidified feed gas stream, a fraction of N_2 or CH_4 (MFC3) was passed through a water container, using a bypass (V5 and V6), to obtain the desired relative humidity content (RH = 11 and 21 vol %) before being mixed with the other components of the gas mixture. The relative humidity present in the gas stream was confirmed using a Vaisala thermohygrometer, equipped with a HM42 probe, placed on the retentate stream, outside of the oven. The membranes to be tested were properly conditioned at the desired water activity, as described in Section 2.3, for $a_w = 0.11$ and $a_w = 0.21$, prior to the experiments. All experiments and calculations were carried out following the procedure described in Section 2.4.2.

3. Results and discussion

In this work, gas permeation experiments were performed using two different systems, to evaluate different parameters. First, the effect of water activity in the MMIMs structures was evaluated by single gas permeation experiments, with dry gases (section 3.1). The objective was to understand how a specific water activity/water content inside the membrane can affect its structure and, consequently, its gas transport properties without the influence of other parameters (humidity of the gas stream, type of gas mixture, etc.). Due to the short duration of these experiments (between 1 and 2 h, with CO_2 being the fastest gas to be permeated), it was assumed that the water activity inside the membrane does not change significantly during each test. Due to the material of the permeation cells used (stainless steel), it was not possible to measure the weight of the different membranes, since the iongel layer was fragile and usually cracked when opening the permeation cell.

In the second part (section 3.2), gas mixtures permeation experiments were performed, considering three variables: temperature, pressure, and RH in the gas stream. In this case, besides the water activity inside the MMIMs (that were also pre-equilibrated), the influence of a specific relative humidity in the gas stream, as well as temperature and pressure were evaluated.

3.1. Effect of water activity on pure gas permeation

3.1.1. Gas permeability

Fig. 4 displays the pure CO_2 permeability of the neat PEGDA-80 TFSI and respective MMIMs containing azo-POPs, equilibrated at different water activities. In this way, this section discusses the impact of the presence of water content inside the structure of the membranes. The CO_2 permeability greatly increased from $a_w = 0$ to $a_w = 0.21$, further decreasing at higher a_w. Similar to what was observed in our previous work ($a_w = 0$) [41], the MMIM containing azo-POP-1 presented the highest CO_2 permeability, regardless of the a_w value, while the neat PEGDA-80 TFSI iongel showed the lowest. This means that the azo-POPs incorporated in the iongels were able to maintain their performance even at different water activities inside the iongel structure, still acting as enhancers of the gas permeability. The neat PEGDA-80 TFSI iongel presented a CO_2 permeability of around 62 Barrer for $a_w = 0$, which

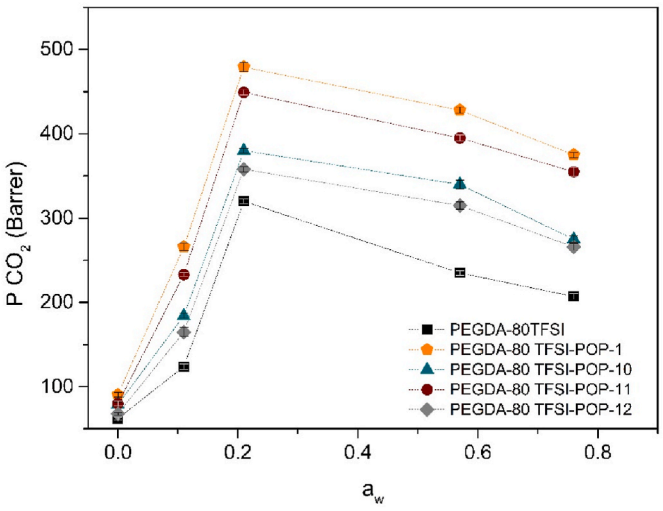

Fig. 4. CO_2 permeability obtained for the neat and mixed matrix iongel membranes as a function of the water activity (a_w).

increased to 320 Barrer at $a_w = 0.21$ and then decreased down to 207 Barrer at higher values of a_w. The CO_2 permeability of the PEGDA-80 TFSI-0.5 POP-1 increased from 91 Barrer for $a_w = 0$ up to 479 Barrer at $a_w = 0.21$, further decreasing down to 375 Barrer at $a_w = 0.76$. In fact, the CO_2 diffusion is expected to increase with increasing a_w, which could be primarily associated with the absorption of water molecules in the polymer matrix [45]. At low a_w, the water molecules are more likely to interact with the polymer rather than with other water molecules, behaving as a plasticizing agent, increasing the free volume in the membrane and, consequently, the gas diffusion. On the other hand, higher a_w (between 0.57 and 0.76), were found to counter this effect, by significantly decreasing the CO_2 permeability [45]. This phenomenon can be attributed to a reduction in diffusivity when the water molecules started to aggregate, creating water clusters that occupy the free volume of the polymer. This hinders the transport of gas species since the water clusters provide a significant obstruction to gas diffusion [46]. As the a_w increased, more water molecules are likely to be absorbed leading to the formation of aggregates, as long as the membrane was able to swell and accommodate such water clusters [45]. Also, the CO_2 solubility is much higher in the iongel matrix comprising the IL [C_2mim][TFSI] and PEGDA than in water (S $CO_2 = 0.76$ cm^3 (STP) cm^{-3} atm^{-1} at 298 K), which also contributed to the observed decrease in the iongels permeability at higher a_w [47]. Overall, the highest increase in CO_2 permeability was achieved with the MMIMs containing azo-POP-1 and azo-POP-11, since these were also the most hydrophilic materials, as shown in our previous work, while the less hydrophilic iongel (PEGDA-80 TFSI) showed the lowest increase in permeability, when compared to the results obtained in the dry state ($a_w = 0$) [41].

Compared to other poly(ethylene glycol)-based membranes (a polymer structurally similar to PEGDA), that also present a hydrophilic nature, the results obtained in this work are similar or higher than those reported in literature [48–51].

Overall, it can be concluded that the presence of water, at low concentrations, can benefit the CO_2 transport of the studied iongel membranes, particularly when azo-POPs are incorporated in the matrix.

3.1.2. Ideal selectivity

Fig. 5 a) and b) displays, respectively, the CO_2/N_2 and CO_2/CH_4 ideal selectivities of the neat iongel and MMIMs containing azo-POPs, as a function of the water activity. Similar to what was observed for the CO_2 permeability, the ideal selectivities increased with an increase in the a_w (up to 0.21) for all the studied iongel membranes. The solubility of CO_2 in water (3.4×10^{-4} mol m^{-3} Pa^{-1}) is considerably higher than that of N_2 (6.4×10^{-6} mol m^{-3} Pa^{-1}) and CH_4 (1.45×10^{-5} mol m^{-3} Pa^{-1}) [47]. These differences contributed to an increase in the CO_2 permeability, which was more significant than for the other less soluble gases (N_2 and CH_4) and thus, ideal selectivity increased. It should also be noted that the azo functional groups can act as selective binding sites for CO_2, hence the MMIMs containing azo-POPs presented higher ideal selectivities compared to the neat PEGDA-80 TFSI iongel membrane. On the other hand, as the a_w increased (from 0.21 to 0.76), there was a notorious decrease in the ideal selectivity for both gas separations. This can be attributed to the clustering effect caused by the presence of more water molecules in the structure that hindered the gas diffusivity. The presence of a higher water content also decreased the gas solubilities because the studied gas species are less soluble in water that in the iongel matrix. Considering that CO_2 has the highest solubility coefficient among all the studied gases, CO_2 will suffer a higher decrease in solubility, which coupled with the decrease in diffusivity, resulted in the observed loss of ideal selectivity.

3.2. Binary gas mixture permeation experiments

Taking into account not only the results of the pure gas permeation experiments previously obtained [41], but also the ones presented in section 3.1 regarding the effect of the water activity on the iongels pure

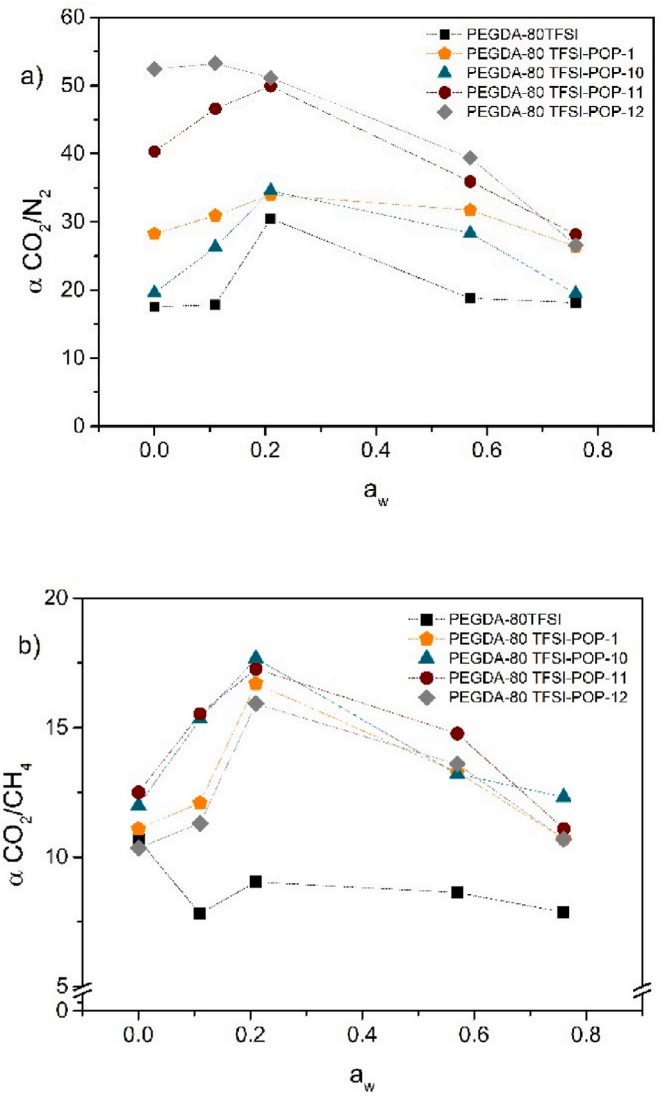

Fig. 5. (a) CO_2/N_2 and (b) $CO2/CH_4$ ideal selectivities of the neat and mixed matrix iongel membranes as a function of the water activity (a_w).

gas permeation, the MMIMs containing azo-POP-1 and azo-POP-11 were selected and evaluated under mixed and humidified gas conditions, for CO_2/N_2 and CO_2/CH_4 separations. Regarding CO_2/N_2 separation, the influence of temperature (303, 323 and 353 K), pressure (2 and 4 bar), gas composition (5–30 vol% CO_2), and RH (11 and 21%) was studied. Additionally, the influence of pressure (2 and 4 bar), gas composition (10–40 vol% CO_2) and relative humidity (11 and 21%) was assessed for the CO_2/CH_4 separation. The results obtained as a function of the vol% CO_2, temperature, pressure and relative humidity for both separations can be found in ESI (Tables S1–S12).

The influence of gas composition on the CO_2/N_2 and CO_2/CH_4 separation performance of the neat iongel and MMIMs containing azo-POP-1 and azo-POP-11 can be perceived from the results presented in Tables S1–S3 and Tables S4–S6 of ESI. Overall, the CO_2 permeability in the CO_2/N_2 binary gas mixture is not significantly influenced by the variation in the feed gas composition between 5 and 15 vol% CO_2. However, at 30 vol%, the CO_2 permeability decreases for all studied iongel membranes. For the CO_2/CH_4 separation, the CO_2 permeability does not present a significant dependence on the feed gas composition.

3.2.1. Effect of temperature

The influence of temperature on the CO_2/N_2 separation of the

studied iongel membranes, with a CO_2 feed composition of 15 vol%, can be found in Table 4. For all iongel membranes, regardless of the experimental pressure, the CO_2 permeability increases with increase in temperature. At 2 bar, the CO_2 permeability increases from 115 Barrer at 303 K to 127 Barrer for the PEGDA-80 TFSI iongel membrane, at 353 K, while the MMIM containing azo-POP-1 presents a CO_2 permeability ranging from 144 to 172 Barrer, under the same experimental conditions. These findings are in agreement with what was previously observed [41], i.e. the MMIMs containing azo-POP-1 had the highest CO_2 permeability, while the neat PEGDA-80TFSI membrane presented the lowest, confirming that even at higher temperatures, the iongel containing azo-POP-1 presents a better separation performance. The same tendency was observed at 4 bar, where the CO_2 permeability consecutively increased with increasing temperature. Higher temperatures lead to an increase in the average kinetic energy and, consequently, in the movement of the gas molecules, improving the rate of diffusion [13,52]. Similar results have also been reported in the literature [52–54].

The permeation of gases through a dense membrane can be considered as an activated process, usually following an Arrhenius type temperature-dependent equation, as follows [55]:

$$P = P_0 \cdot e^{-\frac{E_a}{RT}} \quad (7)$$

Where P is the permeability (cm^3(STP) cm cm^{-2} s^{-1} $cmHg^{-1}$), P_0 is the pre-exponential factor (cm^3(STP) cm cm^{-2} s^{-1} $cmHg^{-1}$), E_a is the activation energy (kJ mol^{-1}), R is the ideal gas constant (kJ mol^{-1} K^{-1}) and T is the temperature (K). To investigate the temperature dependence of the CO_2 permeability, the activation energy was calculated, by plotting $ln\ P$ as a function of $1/T$ for every composition, and the mean values are provided in Table 5. It can be seen that the activation energies obtained for the MMIMs containing azo-POPs were higher than those of the neat PEGDA-80 TFSI iongel. This means that the MMIMs were more sensitive to temperature variations, which was probably attributed to the temperature-dependent intrinsic properties of the azo-functional groups of the POP structure. In fact, previous studies showed that the separation performance, particularly for CO_2/N_2, achieved with azo-POPs can be enhanced when the temperature increases [56]. Monte Carlo simulations evidenced that there is an entropic loss of N_2 gas molecules upon binding, which is more relevant as the temperature increases [56]. Even though the concentration of azo-POP in the iongel membranes is low, it is possible that this factor also contributes to a higher sensitivity to temperature from the MMIMs.

The effect of temperature on the CO_2 permeability presents two contradictory effects: on one hand, it is known that the CO_2 solubility decreases with increasing temperature while, on the other hand, the diffusivity increases. This means that the CO_2 permeability was more solubility-controlled at low temperatures and diffusion-controlled at higher temperatures [52,55].

Although the temperature did not have a significant impact on the CO_2/N_2 selectivity at 2 bar, the MMIMs containing azo-POPs maintained higher separation factors in comparison with the neat PEGDA-80 TFSI iongel, due to the affinity of the azo groups towards CO_2. Moreover, azo-POP-11 provided the highest selectivity, in agreement to what was observed in our previous work [41]. On the other hand, at 4 bar, the selectivity followed the order α (323 K) > α (303 K) > α (353 K). The lower selectivity at 303 K might be explained by a decrease in the CO_2 permeability, at higher pressure, which was not as pronounced for N_2, as it will be discussed in the next section.

Table 4
Effect of temperature and pressure on the CO_2 permeability and CO_2/N_2 selectivity of the neat iongel and MMIMs containing azo-POPs, at 15 vol% CO_2.

Membrane sample	P CO_2 Barrer (α CO_2/N_2)					
	2 bar			4 bar		
	303 K	323 K	353 K	303 K	323 K	353 K
PEGDA-80 TFSI	115 ± 1 (14 ± 1)	124 ± 2 (11 ± 1)	127 ± 2 (12 ± 1)	116 ± 2 (9 ± 1)	147 ± 3 (16 ± 1)	168 ± 2 (6 ± 1)
PEGDA-80 TFSI-0.5 POP-1	144 ± 2 (20 ± 1)	158 ± 2 (19 ± 1)	172 ± 2 (17 ± 1)	140 ± 2 (15 ± 1)	168 ± 2 (16 ± 1)	174 ± 3 (10 ± 1)
PEGDA-80 TFSI-0.5 POP-11	134 ± 3 (24 ± 1)	146 ± 2 (21 ± 1)	163 ± 2 (21 ± 1)	126 ± 2 (13 ± 1)	154 ± 2 (18 ± 1)	178 ± 2 (9 ± 1)

Table 5
Activation energies (E_a) obtained for the neat iongel and MMIMs containing azo-POPs, at different pressures.

Membrane sample	E_a (kJ mol^{-1}) at 2 bar	E_a (kJ mol^{-1}) at 4 bar
PEGDA-80 TFSI	1.56	3.70
PEGDA-80 TFSI-0.5 POP-1	2.97	5.76
PEGDA-80 TFSI-0.5 POP-11	3.22	5.76

3.2.2. Effect of pressure

The results regarding the effect of increasing pressure on the separation performance of the neat PEGDA-80 TFSI iongel and respective MMIMs containing azo-POPs are presented in Tables 4 and 6, for the CO_2/N_2 (xCO_2 = 15 vol%) and CO_2/CH_4 (xCO_2 = 40 vol%) binary gas mixtures, respectively.

At 303 K, the CO_2 permeabilities for both binary gas mixtures slightly decreased as the pressure increased from 2 to 4 bar, except for the PEGDA-80 TFSI iongel in the CO_2/N_2 mixture, where the observed variation is insignificant. The observed decrease in CO_2 permeability at an increased pressure and low temperature (303 K), can be explained by an increase in the competitive sorption between the two gas species in the mixture. It is known that, in gas mixtures, the transport of one gas species across the membrane is directly affected by the presence of other gas components, which is more pronounced for CO_2 due to its lower content in the gas mixture. This is also the reason why, in general, the CO_2/N_2 selectivity decreased at higher pressure, regardless of the temperature (except for a random variation observed for the PEGDA-80 TFSI at 323 K). In what concerns the CO_2/CH_4 gas mixture, the increase in pressure from 2 to 4 bar did not have a significant impact in the gas selectivity.

Looking at the results obtained for the CO_2/N_2 gas mixture (Table 4), the CO_2 permeability obtained at 4 bar and 323 and 353 K increased, when compared to the values obtained at 303 K. The decrease in permeability observed at low temperature was counteracted by an increase in temperature and consequently increase in gas diffusion. In all cases, the CO_2 permeability as well as both CO_2/N_2 and CO_2/CH_4 selectivities were considerably higher for the MMIMs containing azo-POPs, especially for azo-POP-1. For instance, at 15 vol% CO_2, the highest CO_2 permeability of 174 Barrer was achieved with the iongel containing azo-POP-1 at 4 bar and 353 K, along with a CO_2/N_2 selectivity of 10. Regarding the CO_2/CH_4 separation, the MMIMs containing azo-POP-1 also reached the highest CO_2 permeability (253 barrer at 2 bar). This was an expected behaviour since this filler presented the highest porosity (porous volume of 0.57 cm^3 g^{-1}), surface area (1100 m^2 g^{-1}) and CO_2 sorption capacity (2.3 mmol g^{-1} at 273 K) [41].

Table 6
Effect of pressure on the CO_2 permeability and CO_2/CH_4 selectivity of the neat iongel and MMIMs containing azo-POPs, at 303 K and 40 vol% CO_2.

Membrane sample	P CO_2 Barrer (α CO_2/CH_4)	
	2 bar	4 bar
PEGDA-80 TFSI	207 ± 4 (8 ± 1)	191 ± 2 (7 ± 1)
PEGDA-80 TFSI-0.5 POP-1	253 ± 4 (11 ± 1)	227 ± 3 (10 ± 1)
PEGDA-80 TFSI-0.5 POP-11	238 ± 2 (11 ± 1)	220 ± 2 (10 ± 1)

3.2.3. Effect of relative humidity (RH)

Fig. 6 a) and b) and Fig. 7 a) and b) display the effect of the presence of humidity on the CO_2/N_2 and CO_2/CH_4 separations, respectively, for the selected iongel membranes. It is worth mentioning that the tested iongel membranes were pre-equilibrated at the desired water activity, prior to the permeation experiments, as described in section 2.3. The permeability values obtained at RH of 11 and 21% were compared with the results obtained for the dry binary gas mixtures, at 15 vol% CO_2 for CO_2/N_2 and 40 vol% CO_2 for CO_2/CH_4. For both separations, the CO_2 permeability increased as the RH present in the gas mixture increased, for all tested iongel membranes. The increase in CO_2 permeability with increasing humidity was more significant for the PEGDA-80TFSI-0.5 POP-1 membrane, while the neat iongel displayed the lowest increase. Regarding the CO_2/N_2 separation, the CO_2 permeability obtained for the neat PEGDA-80TFSI iongel at 21% of RH was, on average, 1.5 times higher than that obtained under dry conditions. On the other hand, at 21% of RH, the CO_2 permeability increased around 2.7 times for the MMIM containing azo-POP-1 and around 2.3 times for the one containing azo-POP-11, when compared to the dry mixed gas conditions. This behaviour can be explained by the higher hydrophilicity of the PEGDA-80TFSI-0.5 POP-1 iongel material [41], which resulted in a higher swelling of the membrane, meaning that more water-induced plasticization occurred. Consequently, the gas molecules present in the mixture could diffuse faster and more indiscriminately across the iongel membrane. The neat PEGDA-80 TFSI iongel presented a less hydrophilic character, and even though the CO_2 permeability also increased, it was not as significant as it was for the MMIMs containing azo-POPs. On the other hand, the increase in CO_2 permeability was not so accentuated for the CO_2/CH_4 separation, but maintained the same behaviour, with the PEGDA-80TFSI-0.5 POP-1 membrane reaching the highest CO_2 permeability values.

As it can be seen from Fig. 6 b) and Fig. 7 b), the CO_2/N_2 and CO_2/CH_4 selectivities, respectively, obtained under humified conditions were visibly lower than those achieved with the dry binary gas mixtures. As a result of the hydrophilic character of the studied membranes and consequent swelling of the materials in the presence of humidity, the diffusion rate of the gas molecules present in the mixture was enhanced. Moreover, CO_2 is the smallest gas molecule tested in the gas mixture, which means that it should be least affected by the changes in the membrane free volume, contrary to what happens with N_2 and CH_4, leading to a decrease of selectivity [14]. For both separations, the PEGDA-80TFSI-0.5 POP-1 membrane, which was the most hydrophilic membrane and contained the azo-POP with the highest porosity, showed the most marked decrease in selectivity, when compared to that of the remaining iongels. For the CO_2/N_2 separation, the selectivity of the PEGDA-80 TFSI-0.5 POP-1 membrane decreased from around 19, under dry conditions, down to 6 when the RH increased, while for CO_2/CH_4 it decreased from 12 to 3, on average. On the other hand, the neat iongel membrane was the least affected by variations on the RH percentage since its selectivity decreased from 13 to 5 for the CO_2/N_2 separation and from around 10 to 6 for CO_2/CH_4.

4. Conclusions

When considering the use of membranes for gas separation applications, the realistic operating conditions (e.g., gas composition, temperature, pressure, water vapour) of the process are a key-factor to determine the stability, performance and suitability of the chosen materials. Evaluating the separation performance of membranes under pure gas conditions with low temperature and pressure can result in an unrealistic assessment of the true potential of the materials. Bearing this in mind, the influence of temperature, pressure, and RH on the CO_2/N_2 and CO_2/CH_4 gas separations of MMIMs containing azo-POP-1 and azo-POP-11 was assessed in this work. First, MMIMs containing four different azo-POPs were subjected to different saturated salt solutions, revealing that at lower a_w (up to 0.21) both single CO_2 permeabilities and CO_2/N_2 and CO_2/CH_4 ideal selectivities were improved. Conversely, higher values of a_w (up to 0.76) resulted in significantly lower single CO_2 permeability and ideal selectivities, due to a decrease of gas diffusivity and solubility. It is expected that, at higher values of water activity, water molecules start to aggregate, hindering the transport of gas molecules across the iongel matrix. Additionally, gas molecules are less soluble in water than in the iongel membrane comprising IL and PEGDA.

From the binary gas mixtures permeation experiments, it was found that increasing temperature promotes higher CO_2 permeability, while the CO_2/N_2 selectivity was not significantly impacted. It was also observed that, at low temperature (303 K), the CO_2 permeability decreases with increasing pressure (from 2 to 4 bar), which was not observed at higher temperatures (323 and 353 K). In the presence of water in the gas feed stream, the CO_2 permeability is significantly increased, due to the water-induced plasticization of the iongel material, which also led to a considerable decrease in both CO_2/N_2 and CO_2/CH_4 selectivities.

Under both dry and humidified gas conditions, the MMIMs containing azo-POP-1 and azo-POP-11 maintained a higher CO_2 permeability and selectivity, when compared to those of the neat iongel, due the increased porosity and higher CO_2 affinity attributed to the presence of azo functional groups in the POP structure.

Overall, it is clear that different experimental conditions can have a significant impact on the separation performance of the iongel

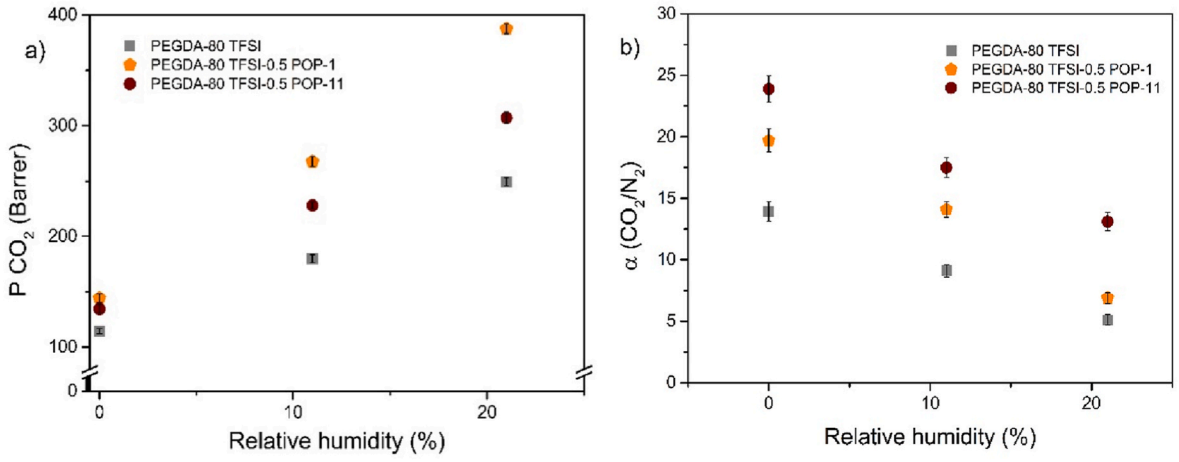

Fig. 6. Effect of relative humidity on the (a) CO_2 permeability and (b) CO_2/N_2 selectivity of the neat iongel and MMIMs containing azo-POPs, at 2 bar, 303 K and 15 vol% CO_2.

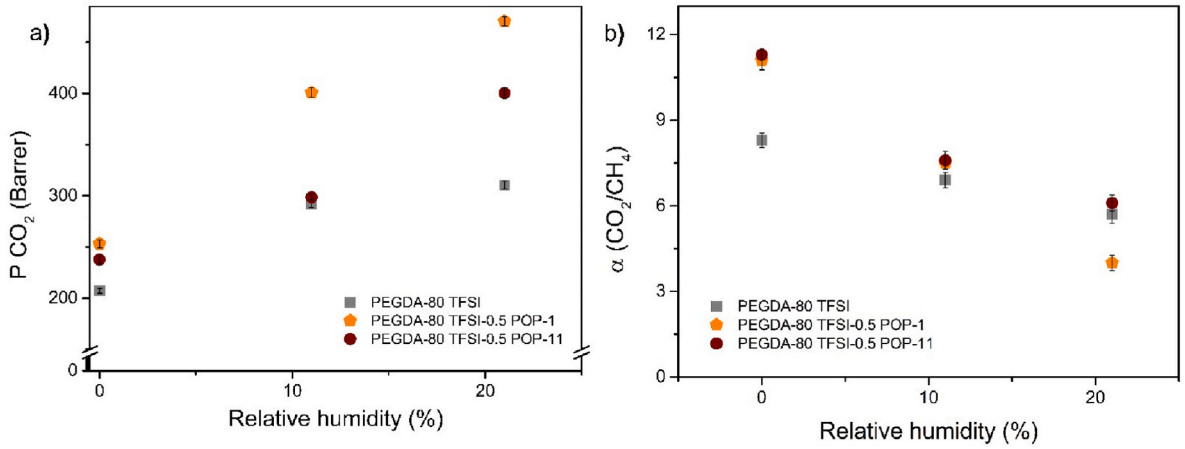

Fig. 7. Effect of relative humidity on the (a) CO_2 permeability and (b) CO_2/CH_4 selectivity of the neat iongel and MMIMs containing azo-POPs, at 2 bar, 303 K and 40 vol% CO_2.

membranes and the obtained results can greatly differ from those obtain with pure gases and low temperatures and pressures. Although the main goal of this work was achieved (to assess the influence of different experimental conditions on the separation performance of MMIMs), further studies should be undertaken to evaluate the long-term stability of these materials under the relevant experimental conditions.

Author contributions

Conceptualization: L. A. Neves, L. C. Tomé;, J. G. Crespo; Investigation: A. R. Nabais, P. Ortiz-Albo, J. X. Zhou; Visualization: A. R. Nabais; Writing - original draft: A. R. Nabais; Writing - review and editing: L. A. Neves, L. C. Tomé;, J. G. Crespo, P. Ortiz-Albo, J. X. Zhou, D. Mecerreyes, M. Huang; Supervision: L. A. Neves, L. C. Tomé;, J. G. Crespo; Resources: L. A. Neves, L. C. Tomé;, D. Mecerreyes.

Declaration of competing interest

The authors declare that they have no known competing financial interests or personal relationships that could have appeared to influence the work reported in this paper.

Data availability

Data will be made available on request.

Acknowledgements

Ana R. Nabais, Paloma Ortiz-Albo and Liliana C. Tomé acknowledge *Fundação para a Ciência e a Tecnologia* (FCT/MCTES) for financial support through PhD grants (SFRH/BD/136963/2018 and SFRH/BD/139389/2018), and assistant researcher contract under Scientific Employment Stimulus (2020.01555.CEECIND), respectively. This work was supported by Associate Laboratory for Green Chemistry - LAQV (UIDB/50006/2020 and UIDP/50006/2020), which is also financed by national funds from FCT/MCTES.

Appendix A. Supplementary data

Supplementary data to this article can be found online at https://doi.org/10.1016/j.memsci.2023.121938.

References

[1] A. Brunetti, F. Scura, G. Barbieri, E. Drioli, Membrane technologies for CO2 separation, J. Membr. Sci. 359 (2010) 115–125, https://doi.org/10.1016/j.memsci.2009.11.040.
[2] M. Rezakazemi, A. Ebadi Amooghin, M.M. Montazer-Rahmati, A.F. Ismail, T. Matsuura, State-of-the-art membrane based CO2 separation using mixed matrix membranes (MMMs): an overview on current status and future directions, Prog. Polym. Sci. 39 (2014) 817–861, https://doi.org/10.1016/j.progpolymsci.2014.01.003.
[3] R.W. Baker, B.T. Low, Gas separation membrane materials: a perspective, Macromolecules 47 (2014) 6999–7013, https://doi.org/10.1021/ma501488s.
[4] E. Favre, Membrane separation processes and post-combustion carbon capture: state of the art and prospects, Membranes 12 (2022), https://doi.org/10.3390/membranes12090884.
[5] B.P. Spigarelli, S.K. Kawatra, Opportunities and challenges in carbon dioxide capture, J. CO2 Util. 1 (2013) 69–87, https://doi.org/10.1016/j.jcou.2013.03.002.
[6] S.D. Kenarsari, D. Yang, G. Jiang, S. Zhang, J. Wang, A.G. Russell, Q. Wei, M. Fan, Review of recent advances in carbon dioxide separation and capture, RSC Adv. 3 (2013) 22739–22773, https://doi.org/10.1039/c3ra43965h.
[7] R. Khalilpour, K. Mumford, H. Zhai, A. Abbas, G. Stevens, E.S. Rubin, Membrane-based carbon capture from flue gas: a review, J. Clean. Prod. 103 (2015) 286–300, https://doi.org/10.1016/j.jclepro.2014.10.050.
[8] A. Brunetti, E. Drioli, Y.M. Lee, G. Barbieri, Engineering evaluation of CO2 separation by membrane gas separation systems, J. Membr. Sci. 454 (2014) 305–315, https://doi.org/10.1016/j.memsci.2013.12.037.
[9] R.W. Baker, K. Lokhandwala, Natural gas processing with membranes: an overview, Ind. Eng. Chem. Res. 47 (2008) 2109–2121, https://doi.org/10.1021/ie071083w.
[10] T.E. Rufford, S. Smart, G.C.Y. Watson, B.F. Graham, J. Boxall, J.C. Diniz da Costa, E.F. May, The removal of CO 2 and N 2 from natural gas: a review of conventional and emerging process technologies, J. Pet. Sci. Eng. 94–95 (2012) 123–154, https://doi.org/10.1016/j.petrol.2012.06.016.
[11] L. Deng, M.B. Hägg, Techno-economic evaluation of biogas upgrading process using CO2 facilitated transport membrane, Int. J. Greenh. Gas Control 4 (2010) 638–646, https://doi.org/10.1016/j.ijggc.2009.12.013.
[12] S.R. Reijerkerk, K. Nijmeijer, C.P. Ribeiro, B.D. Freeman, M. Wessling, On the effects of plasticization in CO2/light gas separation using polymeric solubility selective membranes, J. Membr. Sci. 367 (2011) 33–44, https://doi.org/10.1016/j.memsci.2010.10.035.
[13] E. Lasseuguette, R. Malpass-Evans, M. Carta, N.B. McKeown, M.C. Ferrari, Temperature and pressure dependence of gas permeation in a microporous Tröger's base polymer, Membranes 8 (2018) 1–11, https://doi.org/10.3390/membranes8040132.
[14] J.D. Moon, H. Borjigin, R. Liu, R.M. Joseph, J.S. Riffle, B.D. Freeman, D.R. Paul, Impact of humidity on gas transport in polybenzimidazole membranes, J. Membr. Sci. 639 (2021), 119758, https://doi.org/10.1016/j.memsci.2021.119758.
[15] L.C. Tomé, I.M. Marrucho, Ionic liquid-based materials: a platform to design engineered CO2 separation membranes, Chem. Soc. Rev. 45 (2016) 2785–2824, https://doi.org/10.1039/c5cs00510h.
[16] K. Friess, P. Izák, M. Kárászová, M. Pasichnyk, M. Lanč, D. Nikolaeva, P. Luis, J. C. Jansen, A review on ionic liquid gas separation membranes, Membranes 11 (2021) 1–58, https://doi.org/10.3390/membranes11020097.
[17] H. Gao, L. Bai, J. Han, B. Yang, S. Zhang, X. Zhang, Functionalized ionic liquid membranes for CO2 separation, Chem. Commun. 54 (2018) 12671–12685, https://doi.org/10.1039/c8cc07348a.
[18] C. Cadena, J.L. Anthony, J.K. Shah, T.I. Morrow, J.F. Brennecke, E.J. Maginn, Why is CO2 so soluble in imidazolium-based ionic liquids? J. Am. Chem. Soc. 126 (2004) 5300–5308, https://doi.org/10.1021/ja039615x.

[19] A.P.S. Martins, A.F. De Añastro, J.L. Olmedo-Martínez, A.R. Nabais, L.A. Neves, D. Mecerreyes, L.C. Tomé, Influence of anion structure on thermal, mechanical and CO2 solubility properties of uv-cross-linked poly(Ethylene glycol) diacrylate iongels, Membranes 10 (2020) 46, https://doi.org/10.3390/membranes10030046.
[20] L.C. Tomé, L. Porcarelli, J.E. Bara, M. Forsyth, D. Mecerreyes, Emerging iongel materials towards applications in energy and bioelectronics, Mater. Horiz. 8 (2021) 3239–3265, https://doi.org/10.1039/D1MH01263K.
[21] J. Le Bideau, L. Viau, A. Vioux, Ionogels, ionic liquid based hybrid materials, Chem. Soc. Rev. 40 (2011) 907–925, https://doi.org/10.1039/c0cs00059k.
[22] M.G. Cowan, D.L. Gin, R.D. Noble, Poly(ionic liquid)/ionic liquid ion-gels with high "free" ionic liquid content: platform membrane materials for CO2/light gas separations, Acc. Chem. Res. 49 (2016) 724–732, https://doi.org/10.1021/acs.accounts.5b00547.
[23] X. Yan, S. Anguille, M. Bendahan, P. Moulin, Ionic liquids combined with membrane separation processes: a review, Sep. Purif. Technol. 222 (2019) 230–253, https://doi.org/10.1016/j.seppur.2019.03.103.
[24] A.R. Nabais, L.A. Neves, L.C. Tomé, Mixed-matrix ion gel membranes for gas separation, ACS Appl. Polym. Mater. 4 (2022) 3098–3119.
[25] Y.C. Hudiono, T.K. Carlisle, J.E. Bara, Y. Zhang, D.L. Gin, R.D. Noble, A three-component mixed-matrix membrane with enhanced CO2separation properties based on zeolites and ionic liquid materials, J. Membr. Sci. 350 (2010) 117–123, https://doi.org/10.1016/j.memsci.2009.12.018.
[26] Y.C. Hudiono, T.K. Carlisle, A.L. LaFrate, D.L. Gin, R.D. Noble, Novel mixed matrix membranes based on polymerizable room-temperature ionic liquids and SAPO-34 particles to improve CO 2 separation, J. Membr. Sci. 370 (2011) 141–148, https://doi.org/10.1016/j.memsci.2011.01.012.
[27] Z.V. Singh, M.G. Cowan, W.M. McDanel, Y. Luo, R. Zhou, D.L. Gin, R.D. Noble, Determination and optimization of factors affecting CO2/CH4 separation performance in poly(ionic liquid)-ionic liquid-zeolite mixed-matrix membranes, J. Membr. Sci. 509 (2016) 149–155, https://doi.org/10.1016/j.memsci.2016.02.034.
[28] C.A. Dunn, Z. Shi, R. Zhou, D.L. Gin, R.D. Noble, (Cross-Linked poly(ionic liquid)-ionic liquid-zeolite) mixed-matrix membranes for CO2/CH4 gas separations based on curable ionic liquid prepolymers, Ind. Eng. Chem. Res. 58 (2019) 4704–4708, https://doi.org/10.1021/acs.iecr.8b06464.
[29] E. Kamio, T. Yasui, Y. Iida, J.P. Gong, H. Matsuyama, Inorganic/organic double-network gels containing ionic liquids, Adv. Mater. 29 (2017) 1–8, https://doi.org/10.1002/adma.201704118.
[30] F. Ranjbaran, E. Kamio, H. Matsuyama, Ion gel membrane with tunable inorganic/organic composite network for CO2 separation, Ind. Eng. Chem. Res. 56 (2017) 12763–12772, https://doi.org/10.1021/acs.iecr.7b03279.
[31] E. Kamio, M. Minakata, Y. Iida, T. Yasui, A. Matsuoka, H. Matsuyama, Inorganic/organic double-network ion gel membrane with a high ionic liquid content for CO2 separation, Polym. J. 53 (2021) 137–147, https://doi.org/10.1038/s41428-020-0393-y.
[32] A.R. Nabais, A.P.S. Martins, V.D. Alves, J.G. Crespo, I.M. Marrucho, L.C. Tomé, L. A. Neves, Poly(ionic liquid)-based engineered mixed matrix membranes for CO2/H2 separation, Sep. Purif. Technol. 222 (2019) 168–176, https://doi.org/10.1016/j.seppur.2019.04.018.
[33] A.M. Sampaio, A.R. Nabais, L.C. Tomé, L.A. Neves, Impact of MOF-5 on pyrrolidinium-based poly(ionic liquid)/ionic liquid membranes for biogas upgrading, Ind. Eng. Chem. Res. 59 (2020) 308–317, https://doi.org/10.1021/acs.iecr.9b04206.
[34] A.R. Nabais, R.O. Francisco, V.D. Alves, L.A. Neves, L.C. Tomé, Poly(Ethylene glycol) diacrylate iongel membranes reinforced with nanoclays for CO2 separation, Membranes 11 (2021) 998, https://doi.org/10.3390/membranes11120998.
[35] Z. Yang, H. Zhang, B. Yu, Y. Zhao, Z. Ma, G. Ji, B. Han, Z. Liu, Azo-functionalized microporous organic polymers: synthesis and applications in CO2 capture and conversion, Chem. Commun. 51 (2015) 11576–11579, https://doi.org/10.1039/c5cc03151f.
[36] L. Zou, Y. Sun, S. Che, X. Yang, X. Wang, M. Bosch, Q. Wang, H. Li, M. Smith, S. Yuan, Z. Perry, H.C. Zhou, Porous organic polymers for post-combustion carbon capture, Adv. Mater. 29 (2017) 1–35, https://doi.org/10.1002/adma.201700229.
[37] J. Lu, J. Zhang, Facile synthesis of azo-linked porous organic frameworks via reductive homocoupling for selective CO2 capture, J. Mater. Chem. A. 2 (2014) 13831–13834, https://doi.org/10.1039/c4ta03015j.
[38] J.X. Zhou, X.S. Luo, X. Liu, Y. Qiao, P. Wang, D. Mecerreyes, N. Bogliotti, S.L. Chen, M.H. Huang, Azo-linked porous organic polymers: robust and time-efficient synthesis: via NaBH4-mediated reductive homocoupling on polynitro monomers and adsorption capacity towards aniline in water, J. Mater. Chem. A. 6 (2018) 5608–5612, https://doi.org/10.1039/c8ta00341f.
[39] Z.W. Liu, B.H. Han, Ionic porous organic polymers for CO2 capture and conversion, Curr. Opin. Green Sustain. Chem. 16 (2019) 20–25, https://doi.org/10.1016/j.cogsc.2018.11.008.
[40] A.R. Nabais, L.A. Neves, L.C. Tomé, Mixed-matrix ion gel membranes for gas separation, ACS Appl. Polym. Mater. 4 (2022) 3098–3119, https://doi.org/10.1021/acsapm.1c01737.
[41] A.R. Nabais, S. Ahmed, M. Younis, J. Zhou, F. Freitas, D. Mecerreyes, G.J. Crespo, M. Huang, L.A. Neves, L.C. Tomé, Mixed matrix membranes based on ionic liquids and porous organic polymers for selective CO2 separation, J. Membr. Sci. 660 (2022), 120840, https://doi.org/10.1016/j.memsci.2022.120841.
[42] L. Greenspan, Humidity fixed points of binary saturated aqueous solutions, J. Res. Natl. Bur. Stand. A. Phys. Chem. 81 (1977) 89–96, https://doi.org/10.6028/jres.081A.011.
[43] L.A. Neves, J.G. Crespo, I.M. Coelhoso, Gas permeation studies in supported ionic liquid membranes, J. Membr. Sci. 357 (2010) 160–170, https://doi.org/10.1016/j.memsci.2010.04.016.
[44] E.L. Cussler, Fundamentals of Mass Transfer, third ed., Cambridge University Press, New York, 2009 https://doi.org/10.1017/CBO9780511805134.010.
[45] G.Q. Chen, C.A. Scholes, G.G. Qiao, S.E. Kentish, Water vapor permeation in polyimide membranes, J. Membr. Sci. 379 (2011) 479–487, https://doi.org/10.1016/j.memsci.2011.06.023.
[46] C.A. Scholes, J. Jin, G.W. Stevens, S.E. Kentish, Competitive permeation of gas and water vapour in high free volume polymeric membranes, J. Polym. Sci., Part B: Polym. Phys. 53 (2015) 719–728, https://doi.org/10.1002/polb.23689.
[47] R. Sander, Compilation of Henry's law constants for water as solvent, Atmos. Chem. Phys. 15 (2015) 4399–4981, https://doi.org/10.5194/acp-15-4399-2015.
[48] S. Karimi, E. Firouzfar, M.R. Khoshchehreh, Assessment of gas separation properties and CO2 plasticization of polysulfone/polyethylene glycol membranes, J. Pet. Sci. Eng. 173 (2019) 13–19, https://doi.org/10.1016/j.petrol.2018.10.012.
[49] J. Deng, Z. Dai, J. Yan, M. Sandru, E. Sandru, R.J. Spontak, L. Deng, Facile and solvent-free fabrication of PEG-based membranes with interpenetrating networks for CO2 separation, J. Membr. Sci. 570–571 (2019) 455–463, https://doi.org/10.1016/j.memsci.2018.10.031.
[50] D. Vroulias, E. Staurianou, T. Ioannides, Poly (Ethylene Oxide) -Based Copolymer-IL Composite Membranes for CO 2 Separation, 2023.
[51] S. Bandehali, A. Moghadassi, F. Parvizian, S.M. Hosseini, T. Matsuura, E. Joudaki, Advances in high carbon dioxide separation performance of poly (ethylene oxide)-based membranes, J. Energy Chem. 46 (2020) 30–52, https://doi.org/10.1016/j.jechem.2019.10.019.
[52] B. Zhang, C. Yang, Y. Zheng, Y. Wu, C. Song, Q. Liu, Z. Wang, Modification of CO2-selective mixed matrix membranes by a binary composition of poly(ethylene glycol)/NaY zeolite, J. Membr. Sci. 627 (2021), 119239, https://doi.org/10.1016/j.memsci.2021.119239.
[53] A.S.L. Gouveia, M. Yáñez, V.D. Alves, J. Palomar, C. Moya, D. Gorri, L.C. Tomé, I. M. Marrucho, CO2/H2 separation through poly(ionic liquid)–ionic liquid membranes: the effect of multicomponent gas mixtures, temperature and gas feed pressure, Sep. Purif. Technol. 259 (2021), 118113, https://doi.org/10.1016/j.seppur.2020.118113.
[54] S.A. Gulmus, L. Yilmaz, Effect of temperature and membrane preparation parameters on gas permeation properties of polymethacrylates, J. Polym. Sci., Part B: Polym. Phys. 45 (2007) 3025–3033, https://doi.org/10.1002/polb.
[55] C.K. Yeom, S.H. Lee, J.M. Lee, Study of transport of pure and mixed CO2/N2 gases through polymeric membranes, J. Appl. Polym. Sci. 78 (2000) 179–189, https://doi.org/10.1002/1097-4628(20001003)78:1<179::AID-APP220>3.0.CO;2-Z.
[56] H.A. Patel, S. Hyun Je, J. Park, D.P. Chen, Y. Jung, C.T. Yavuz, A. Coskun, Unprecedented high-temperature CO2 selectivity in N 2-phobic nanoporous covalent organic polymers, Nat. Commun. 4 (2013) 1–8, https://doi.org/10.1038/ncomms2359.